Decomposition of single-source precursors under high-temperature high-pressure to access osmium–platinum refractory alloys

Kirill V. Yusenko,[a,*] Kristina Spektor,[b] Saiana Khandarkhaeva,[c] Timofey Fedotenko,[d] Anna Pakhomova,[e] Ilya Kupenko,[f] Arno Rohrbach,[f] Stephan Klemme,[f] Wilson A. Crichton, Tatyana V. Dyachkova,[g] Alexander P. Tyutyunnik,[g] Yurii G. Zainulin,[g] Leonid S.Dubrovinsky,[c] Sergey A. Gromilov[h,i]

[a]BAM Federal Institute of Materials Research and Testing, Richard-Willstätter Str. 11, D-12489 Berlin, Germany
[b]ESRF-The European Synchrotron 71 Avenue des Martyrs, 38000, Grenoble, France
[c]Bayerisches Geoinstitut, Universität Bayreuth, D-95440 Bayreuth, Germany
[d]Material Physics and Technology at Extreme Conditions, Laboratory of Crystallography, University of Bayreuth, D-95440 Bayreuth, Germany
[e]Photon Sciences, Deutsches Elektronen-Synchrotron, Notkestrasse 85, D-22607 Hamburg, Germany
[f]Institut für Mineralogie, Westfälische-Wilhelms-Universität Münster, Corrensstrasse 24, 48149 Münster, Germany
[g]Institute of Solid State Chemistry, Pervomaiskaia str. 91, 620990 Ekaterinburg, Russia
[h]Nikolaev Institute of Inorganic Chemistry, Lavrentiev ave. 3, 630090 Novosibirsk, Russia
[i]Novosibirsk State University, Pirogova str. 2, 630090 Novosibirsk, Russia

*Corresponding author: BAM Federal Institute of Materials Research and Testing, Richard-Willstätter Str. 11, D-12489 Berlin, Germany; kirill.yusenko@bam.de

Thermal decomposition of $(NH_4)_2[Os_xPt_{1-x}Cl_6]$ as single-source precursors for Os-Pt binary alloys has been investigated under ambient and high pressure up to 40 GPa. Thermal decomposition of mixed-metal $(NH_4)_2[Os_xPt_{1-x}Cl_6]$ precursor in hydrogen atmosphere (reductive environment) under ambient pressure results in formation of *β-trans*-$[Pt(NH_3)_2Cl_2]$ and *α-trans*-$[Pt(NH_3)_2Cl_2]$ crystalline intermediates as well as single and two-phase Os—Pt binary alloys. For the first time, direct thermal decomposition of coordination compound under pressure has been investigated. A formation of pure metallic alloys from single-source precursors under pressure has been shown. Miscibility between *fcc*- and *hcp*-structured alloys has been probed up to 50 GPa by *in situ* high-pressure X-ray diffraction. Miscibility gap between *fcc*- and *hcp*-structured alloys does not change its positions with pressure up to at least 50 GPa.

Keywords: osmium, platinum, alloys, phase diagrams, single-source precursors, high-pressure high-temperature.

Introduction

Refractory alloys based on platinum group metals have been proposed as materials for extreme environments such as high mechanical impact, oxidative stress as well as high-temperatures and high-pressures conditions. Phase diagrams, mechanical and functional properties of refractory platinum group alloys were investigated in many details by heating up to their melting temperatures (*i.e.* above 1500–3000 °C). However, investigations under high hydrostatic pressure were performed only for a limited number of binary systems, mainly for Fe—Ru, Ir—Hf, Ir—Os, and Ir—Re [1–5]. Recent investigations suggested high phase stability of refractory metals and their alloys up to extremely high-pressures reaching 1 TPa [6-7]. Such finding makes refractory alloys as possible models for investigation and development of ultra-incompressible materials [8]. Investigation of refractory binaries with hexagonal close packed (*hcp*: Os, Re, Ru) and face centred cubic (*fcc*: Ir, Pt, Rh) refractory metals allowed one to formulate general trend in their phase stability under pressure as follows: along compression the miscibility gap between *hcp* and *fcc* alloys shifts towards the metal with larger atomic volume [9]. Previously we have confirmed this tendency for Ir—Os and Ir—Re alloys, where metals have close atomic volumes and significantly different compressibility (Ir—Os binary alloys) or different atomic volumes and nearly identical compressibility (Ir—Re binary alloys).

Os—Pt binary alloys have relevance not only as refractory constructional system but also as functional materials with high catalytic activity in CO oxidation [10–12]. It should be mentioned that Os—Pt binaries for catalytic and mechanical tests were originally prepared using arc-melting which requires relatively large amount of materials as well as cannot be considered as an effective tool for preparation of supported metallic particles with high porosity. Alternatively, materials for catalytic tests were prepared from water solutions using $NaBH_4$ as reducing agent [13].

In our previous studies, an alternative strategy to access nanoporous refractory alloys from solid or supported single-source precursors has been reported [3–5]. So, Os—Pt alloys can be prepared by reducing a solid single-source precursor in a hydrogen flow according to the following chemical reaction:

$$(NH_4)_2[Os_xPt_{1-x}Cl_6] + 2H_2 \xrightarrow{600\text{-}800\ ^\circ C} Os_xPt_{1-x} + 4HCl + 2NH_4Cl;$$

or through thermal decomposition in inert atmosphere (He, Ar, or N_2):

$$(NH_4)_2[Os_xPt_{1-x}Cl_6] \xrightarrow{600\text{-}900\ ^\circ C} Os_xPt_{1-x} + 2/3N_2 + 16/3HCl + 2/3NH_4Cl.$$

Current strategy allows us to prepare Os—Pt alloys in the whole range of concentrations using relatively low temperatures and further probe their phase stability under high-pressure high-temperature conditions.

In the current study, we report an investigation of Os_xPt_{1-x} alloys prepared from $(NH_4)_2[Os_xPt_{1-x}Cl_6]$ coordination compounds as single-source precursors. Thermal decomposition of the precursors in inert and reductive atmospheres at ambient and high pressure up to 40 GPa has been investigated using *in situ* X-ray diffraction. Phase stability and phase separation of Os_xPt_{1-x} alloys have been investigated under extreme conditions up to 50 GPa and 3000 °C. We report behaviour of Os—Pt binary alloys under high-pressure high-temperature condition to extend our knowledge with a system where both atomic volumes and compressibilities for *fcc*- and *hcp*-structured metals are significantly different. Thermal decomposition of $(NH_4)_2[Os_xPt_{1-x}Cl_6]$ compounds as single-source precursors under high-pressure in inert and reductive environment gave us a possibility to extend our knowledge about behaviour of coordination compounds under extreme conditions as well as to show a possibility to decompose coordination salts under high-pressure without formation of parasitic binary compounds.

Experimental section

Single-source precursors, $(NH_4)_2[Os_xPt_{1-x}Cl_6]$, were crystallized by adding an excess of saturated water solution of NH_4Cl to a mixture of hot concentrated water solutions of $(NH_4)_2[OsCl_6]$ and $(NH_4)_2[PtCl_6]$ (obtained from Acros Organics) [14–15]. Salts were filtered, washed with diluted room temperature water solution of NH_4Cl, absolute ethanol and dried in air. Elemental compositions were confirmed in 10 points using a Hitachi S-4800 Field Emission scanning electron microscope (SEM) equipped with energy dispersive X-ray (EDX) analyser and averaged for 10 points for each sample.

The thermal decomposition of $(NH_4)_2[Os_{0.40}Pt_{0.60}Cl_6]$ at ambient pressure was investigated *in situ* using the powder X-ray diffraction (PXRD) set-up located at the ID11 beamline of the European Synchrotron Radiation Facility (ESRF, Grenoble, France). Samples in powder form were placed in 0.5 mm fused quartz mark tubes (Hilgenberg GmbH, Germany). Capillaries were connected to a 2 vol.% H_2/Ar or pure Ar flow (0.1–0.5 ml/min) and heated with hot air stream from room temperature to 900 °C with a ramp rate of 12 °C/min. Temperature was calibrated using the thermal expansion of the cell parameters for silver powder as an external standard. The wavelength (λ = 0.3086 Å) and sample-to-detector distance were calibrated using CeO_2 powder as external standard. Data were collected every 20 s (approximately every 4 K in the temperature scale) using a Frelon2K 2D flat detector. The data were converted, and diffracted intensities integrated using custom written Python-based algorithm. Temperature dependent PXRD patterns were plotted and analysed using the Powder3D software [16].

High-pressure high-temperature decomposition of $(NH_4)_2[Os_{0.40}Pt_{0.60}Cl_6]$ at 1 GPa has been performed in an end-loaded piston cylinder apparatus installed at the Institut für Mineralogie, WWU Münster [17]. $(NH_4)_2[Os_{0.40}Pt_{0.60}Cl_6]$ powder was enclosed in a 2 mm alumina crucible.

The pressure assembly consisted of a ½-inch talc-Pyrex cylinders, which contained an 8 mm diameter graphite heater with inner parts of crushable Al_2O_3 (TKF GmbH, Kerschenbroich, Germany). Temperature was monitored and controlled with a $W_{97}Re_3$–$W_{75}Re_{25}$ thermocouple. The sample was compressed to 1 GPa with further heating up to 1000 °C. After 80 min under compression and heating, the sample was quenched to room temperature and subsequently decompressed for 2 h.

High-pressure high-temperature decomposition of $(NH_4)_2[Os_{0.40}Pt_{0.60}Cl_6]$ at 8 GPa in H_2 fluid was performed in the large-volume 2000 tons MAVO press in a 6/8 mode with 25 mm tungsten carbide anvils (ID06–LVP beamline, ESRF [18], $\lambda = 0.2254$ Å). A linear pixelated GOS detector was used for *in situ* data collection (sequential exposure of 3.2 seconds at 10 Hz at 32 seconds interval, mounted to intercept the downstream diffraction from the horizontal anvil gap at ~2040 mm distance). The detector-beam normal plane was mechanically corrected for tilt and rotation, the detector position was corrected for zero-offset and calibrated against LaB_6 (SRM660a). For this experiment, the sample was pressed into a pellet (1.4 mm OD, 1.5 mm height) and sealed inside a NaCl capsule (3 mm OD, 3.5 mm height) along with 2 pellets of NH_3BH_3 (ammonia borane, 0.45 mm height, 1.4 mm OD). NH_3BH_3 was employed as a hydrogen source, providing ~6 times molar excess of H_2 fluid with respect to the metals. The sample capsule preparation was handled in an Ar-filled glove box. Afterwards, the NaCl capsule was surrounded with a BN sleeve and along with carbon foil resistance furnace and ZrO_2 plugs was inserted into the 14 mm OEL octahedral Cr:MgO assembly. The octahedron was further positioned between eight 25 mm WC anvils (Hawedia, ha7, 8 mm TEL) equipped with pyrophyllite gaskets. Amorphous SiBCN rods (2 mm OD) and 5 mm wide MgO rectangles served as X-Ray windows in the octahedron and the gaskets along the beam direction. Pressures and temperatures were

estimated using the NaCl *P—V—T* equation of state [19]. The sample was compressed up to 9 GPa and carefully heated to 300 °C to decompose NH_3BH_3 and release H_2. After hydrogen release though the pressure dropped to 8–8.5 GPa. Further heating in H_2 fluid up to 600 °C under *quasi*-constant pressure was done in 60 minutes with further annealing during 1 h. On compression, heating, cooling and decompression PXRD data were simultaneously collected. Two-dimensional images were integrated to one-dimensional intensities as a function of diffraction angle using the FIT2D [20].

High-pressure high-temperature decomposition of $(NH_4)_2[Os_{0.25}Pt_{0.75}Cl_6]$ at 4 GPa and $(NH_4)_2[Os_{0.50}Pt_{0.50}Cl_6]$ at 10 GPa have been performed in a standard toroid-type chamber of a pressure apparatus at the Institute of Solid State Chemistry (Ekaterinburg, Russia) [21]. Powdered salt was pressed inside a graphite crucible with a boron nitride insulation. Stable compact tablets with a diameter of 3 mm were obtained after 3–5 min treatment at 2000 °C and 4 and 10 GPa. Graphite crucibles insulated with *h*-BN were used to avoid any contact of the reaction mixture with oxygen atmosphere. No oxides, nitrides or carbides were detected after high-temperature high-pressure treatment.

High-pressure high-temperature decomposition of $(NH_4)_2[Os_{0.50}Pt_{0.50}Cl_6]$ at 18.5 GPa has been performed in a 1000 t multi-anvil press installed at the Institute of Mineralogy, WWU Münster. 10/4 assemblies were used with chromium-doped MgO octahedra, stepped $LaCrO_3$ furnaces and pyrophyllite gaskets. The assembly was pressure-calibrated at high temperatures using olivine-wadsleyite-ringwoodite phase transitions [17]. The starting powders were encapsulated into polycrystalline crushable Al_2O_3 containers. The experiments were brought up to 18.5 GPa and further heated to 1200 °C at a rate of 10 °C/min and then kept constant for 5 minutes.

Samples were quenched by turning off the power supply, resulting in reducing the temperature to below 420 °C in less than 1 s, and decompressed overnight.

Phase identity of recovered samples was investigated at ambient conditions using PXRD without grinding at ID06-LVP (8 and 18 GPa samples, λ = 0.2296 Å) and ID15B beamlines (8 and 1 GPa samples, λ = 0.4112 Å), as well as at in house STADI-P (Stoe) diffractometer (10 GPa sample, slightly ground) in transmission geometry with a linear mini-PSD detector in the 2θ range 5–120° with a step of 0.02°. Focused $CuK_{\alpha 1}$ (λ = 1.54059 Å) incident beam was obtained using curved Ge(111) monochromator. Polycrystalline silicon (*a* = 5.43075(5) Å) was used as external standard.

High-pressure high-temperature decomposition of $(NH_4)_2[Os_{0.50}Pt_{0.50}Cl_6]$ above 20 GPa has been performed in a membrane Mao-type diamond anvil cell (DAC) with conically supported Boehler Almax type anvils (150 μm culet sizes) at the P02.2. beamline [22], PETRA III, DESY in Hamburg (λ = 0.2907 Å, Perkin Elmer XRD1621 (2048x2048 pixels, 200x200 μm^2) flat panel detector, beam size 3(*v*)×3(*h*) μm^2). A powdered sample was loaded in a hole drilled in the pre-indented rhenium gasket. Pressure was determined using a ruby luminescence. Neon serving as a pressure-transmitting medium was loaded at ∼1.5 kbar using the gas-loading system installed at the beamline. The diffraction images were recorded under continuous ω-rotation of the DAC from -3 to +3° with 6 second acquisition time. After room temperature compression up to 24 GPa, the sample was laser-heated online up to 2000–2300 °C from both sides with simultaneous collection of diffraction images. Temperature was estimated from the black body radiation. Afterwards, cell was compressed at 34 GPa and heated up to 1000–1200 °C, at 40 GPa and up to 1600 °C and finally at 50 GPa and heated up to 850 °C. PXRD for all steps was collected after quenching to room temperature. Quenched unloaded sample was also measured without DAC to

confirm its phase composition. Data were treated and integrated using DIOPTAS software [23]. Unit cell, background, and line-profile parameters for sample and gold internal standard as well as Ne diffraction lines were refined simultaneously using model-free full-profile refinement implemented in JANA2006 software [24].

Results and discussion

Os—Pt alloys under ambient pressure. A peritectic Os—Pt ambient pressure binary phase diagram was investigated using arc-melted samples [25] (Figure 1). Peritectic temperature was estimated at around 1955 °C. The maximal solubilities of Pt in *hcp*-structured (10 at. %) and Os in *fcc*-structured (20 at. %) alloys were obtained by Rudman [26] using high-temperature sintering of fine metallic powders (Table 1). Later, more concentrated alloys were prepared using thermal decomposition of single source precursors: *hcp*–$Os_{0.75}Pt_{0.25}$ was prepared from $(NH_4)_2[Os_{0.75}Pt_{0.25}Cl_6]$ [14] and *fcc*–$Os_{0.30}Pt_{0.70}$ was obtained from $(NH_4)_2[Os_{0.30}Pt_{0.70}Cl_6]$ [15], which suggests the narrower miscibility gap in the Os—Pt binary metallic system. Of importance, $[Pt(NH_3)_4][OsCl_6]$ or $[Pt(NH_3)_4][OsBr_6]$ were considered as single-source precursors for a single-phase *fcc*–$Os_{0.50}Pt_{0.50}$. However, cell parameters of obtained *equi*-atomic *fcc*-structured alloys were estimated much higher in comparison with other compositions. Recent investigations [29] suggested a metastable nature of obtained *fcc*-$Os_{0.50}Pt_{0.50}$ alloy. Originally formed *fcc*-$Os_{0.50}Pt_{0.50}$ under low temperature (below 600 °C) with further high-temperature annealing decomposes with a formation of *fcc*+*hcp* two-phase mixture.

At room temperature, atomic volumes (V/Z, $Å^3 \cdot atom^{-1}$) of Os—Pt alloys correspond to two polynomial functions:

$$V/Z_{fcc} = 14.68(7) - 3(2)\cdot 10^{-3}\cdot x_{Pt} + 7(1)\cdot 10^{-5}\cdot x_{Pt}^2,$$

$$V/Z_{hcp} = 13.97(4) + 7(7)\cdot 10^{-3}\cdot x_{Pt} + 1(2)\cdot 10^{-4}\cdot x_{Pt}^2;$$

where x_{Pt}, at. % corresponds to the Pt atomic fraction in alloy. V/Z_{fcc} and V/Z_{hcp} correspond to atomic volumes of *fcc*- ($Z = 4$) and *hcp*- ($Z = 2$) structured alloys. Both fits are quite close to the linear function: $V/Z = 13.95(1) + 11.3(3)\cdot10^{-3}\cdot x_{Pt}$. Linear function can be used as a tool to obtain phase composition for two-phase samples with known cell parameters.

Peritectic Os—Pt binary phase diagram can be reproduced based on ideal solutions model (without mixing parameters) using CALPHAD approach realised in PANDAT 8 software [30] with the SGTE v 4.4 thermodynamic database for pure elements [31]. Experimental and modelled phase diagrams are quite close to each other for Pt-rich alloys, but Os-rich part cannot be reproduced.

Os—Pt alloys under high-pressure. Two-phase Os—Pt alloys annealed or formed from single-source precursor under high-pressure represent a miscibility gap in the binary phase diagram under compression. In current study, high-pressure high-temperature annealing up to 3000 °C and 50 GPa has been performed to probe dependence of a miscibility between *fcc*- and *hcp*-structured alloys on pressure (Table 2, Figure 2). All samples were investigated after quenching and recovering under ambient pressure. According to our previous knowledge, quenching and pressure unload do not change phase composition and phase amounts and recovered samples correspond to high-pressure situation [3–5]. According to our previous experimental observations for Ir—Os and Ir—Re binaries, miscibility gap in peritectic binary systems should shift towards metal with higher atomic volume [3–5]. In the mentioned binary systems, metals have close atomic volumes (14.155 *vs*. 13.971 $Å^3\cdot atom^{-1}$) and significantly different compressibility (341 *vs*. 399 GPa) for Ir—Os binary alloys or different atomic volumes (14.155 *vs*. 14.730 $Å^3\cdot atom^{-1}$) and very close compressibility values (341 *vs.* 353 GPa) for Ir—Re binary alloys. But on the contrary, Pt and Os have significantly different atomic volumes (15.094 *vs.* 13.971 $Å^3\cdot atom^{-1}$) and bulk moduli (273.5 *vs.*

399 GPa) [7, 32]. For Os—Pt alloys miscibility gap does not change with pressure or just slightly shifts towards osmium below 50 GPa, which suggests high structural stability of discussed refractory binary system.

Two-phase alloys obtained by thermal decomposition of $(NH_4)_2[Os_xPt_{1-x}Cl_6]$ precursors in inert conditions (10 GPa, 18 GPa and above) and in hydrogen fluid (8.5 GPa) show similar results which suggests formation of equilibrium phases under all observed pressures. At the same time, annealing of pre-synthetized metallic powders as well as precursors under relatively low hydrostatic pressure (below 2 GPa) results in a formation of alloys with less amount of second metal, which might be a result of low inter-diffusion or separate formation of metals in the thermal decomposition process. In the sample annealed at 18 GPa, cell parameters for hexagonal phase are masked under diffraction lines of assembly. As a result, only cubic phase can be refined.

Data obtained under low pressure (below 2.5 GPa) has low reproducibility due to a number of experimental factors. Samples releases relatively large number of volatile products which provoke large stress and gradients in large assemblies. As a result, large assemblies should have high temperature and pressure gradients upon heating. Short reaction and temperature annealing times (several minutes) probably do not give equilibrium samples. High-pressure experiments (above 10 GPa) can be considered as more reproducible due to relatively small sample volumes with fast reaction times and low temperature and pressure gradients.

Pressure dependence of phase diagrams for refractory ultra-incompressible metals were never modelled using CALPHAD as well as ab initio approaches. Nevertheless, our data gives an experimental basis for further construction of such phase diagrams using compressibility data for pure metals and their alloys as well as pressure dependence of miscibility gaps in binary systems. We hope to perform theoretical modelling to support our experimental studies in the nearest future.

Formation of Os—Pt alloys from single-source precursors. All binary Os—Pt alloys were prepared from $(NH_4)_2[Os_xPt_{1-x}Cl_6]$ as single-source precursors. In all previous reports, alloys were prepared under ambient pressure and further annealed under compression. However, single-source precursor already contains reducing agent and can be thermally decomposed under pressure with easy formation of metallic alloys. In other words, thermal decomposition of the precursor under compression also results in a formation of equilibrium metallic composition and can be used to probe miscibility gap in the phase diagram under high-pressure similarly to ambient pressure trials.

To shed the light on the thermal behaviour of $(NH_4)_2[Os_xPt_{1-x}Cl_6]$ bimetallic compound, its thermal decomposition in hydrogen and helium under ambient pressure as well as in hydrogen fluid under compression (8.5–9 GPa) was monitored *in situ* using X-ray diffraction.

Previously, thermal decomposition of $(NH_4)_2[PtCl_6]$ in inert atmosphere (He) and $(NH_4)_2[OsCl_6]$ in reducing (H_2 in Ar) and inert (He) atmospheres were investigated using *in situ* PXRD and EXAFS [34]. It has been proposed that both compounds decompose with a formation of several intermediates which can be detected using spectroscopic techniques but invisible in PXRD. *trans*- and/or *cis*-$[Pt(NH_3)_2Cl_2]$ and polymeric $\{OsCl_4\}_n$ were proposed as key intermediates. However, several previous *ex situ* investigations of $(NH_4)_2[PtCl_6]$ did not give much insight into its thermal decomposition in H_2 flow while the most data were obtained in an inert gas atmosphere [34–38].

In the current study, we chose $(NH_4)_2[Os_{0.40}Pt_{0.60}Cl_6]$ as representative example of bimetallic compounds within $(NH_4)_2[Os_xPt_{1-x}Cl_6]$ series. Metallic products as well as thermal decomposition process seem to be similar for all other compositions. Similar assumption was used for our previous studies of thermal decomposition of $(NH_4)_2[Ir_xOs_{1-x}Cl_6]$ and $(NH_4)_2[Ir_xRe_{1-x}Cl_6]$ in H_2-flow where

Ir(III)-containing intermediate was detected [4, 5]. Figure 3 summarizes temperature-dependent PXRD data collected upon heating in inert and reducing atmosphere under ambient pressure. In Ar flow (inert atmosphere), $(NH_4)_2[Os_{0.40}Pt_{0.60}Cl_6]$ forms directly single-phase *fcc*-$Os_{0.40}Pt_{0.60}$ above 400 °C. Single-phase alloy decomposes with a formation of *fcc*+*hcp* mixture with further heating (Table 2). Such decomposition of $(NH_4)_2[Os_{0.40}Pt_{0.60}Cl_6]$ without a formation of any crystalline intermediates detectable by PXRD was expected based on data obtained for pure $(NH_4)_2[PtCl_6]$ and $(NH_4)_2[OsCl_6]$.

Surprisingly, thermal decomposition of $(NH_4)_2[Os_{0.40}Pt_{0.60}Cl_6]$ in 2 vol.% H_2/Ar flow occurs with a formation of several intermediates. Above 200 °C, $(NH_4)_2[Os_{0.40}Pt_{0.60}Cl_6]$ forms β-*trans*-$[Pt(NH_3)_2Cl_2]$ (isostructural with β-*trans*-$[Pd(NH_3)_2Cl_2]$: *Pbam, a* = 8.1415(6), *b* = 8.1459(7), *c* = 7.7888(5) Å, *Z* = 4 [39]), NH_4Cl and *fcc*-structured metallic phase. Further heating above 250 °C results in the transformation of β-*trans*-$[Pt(NH_3)_2Cl_2]$ intermediate to α-*trans*-$[Pt(NH_3)_2Cl_2]$ (isostructural with α-*trans*-$[Pd(NH_3)_2Cl_2]$: $P\bar{1}$, *a* = 6.299(4), *b* = 6.554(4), *c* = 6.819(4) Å, α = 100.900(18)°, β = 102.82(3)°, γ = 102.068(12)°, *Z* = 2 [40]). Above 300 °C, only *fcc*–$Os_{0.40}Pt_{0.60}$ can be detected. Further annealing results in a formation of *fcc* + *hcp* alloys mixture. It is important to note that *cis*-$[Pt(NH_3)_2Cl_2]$ was not detected as crystalline product at any temperatures. Both polymorphs, β-*trans*-$[Pt(NH_3)_2Cl_2]$ and α-*trans*-$[Pt(NH_3)_2Cl_2]$, are well-known for Pd but were not previously described for Pt. Both Pd polymorphs, β-*trans*-$[Pd(NH_3)_2Cl_2]$ and α-*trans*-$[Pd(NH_3)_2Cl_2]$, were synthetized and characterized structurally. α-*trans*-$[Pd(NH_3)_2Cl_2]$ is less stable and easily irreversibly transforms to β-*trans*-$[Pd(NH_3)_2Cl_2]$ with heating in a solid-state. It seems that less symmetric structure, α-*trans*-$[Pt(NH_3)_2Cl_2]$, is more stable. Since only the strongest diffraction lines characteristic for Pt-containing intermediates were detected, detailed crystal

structure of detected intermediate crystalline phases could not be extracted from such relatively poor X-ray diffraction data.

Thermal decomposition of $(NH_4)_2[Os_{0.40}Pt_{0.60}Cl_6]$ in hydrogen flow under ambient pressure starts already at 200 °C and can be schematically summarized as follows:

$$(NH_4)_2[Os_{0.40}Pt_{0.60}Cl_6] \rightarrow \beta\text{-}trans\text{-}[Pt(NH_3)_2Cl_2] + NH_4Cl + fcc\text{–}Pt_xOs_{1-x} + \text{“}OsCl_4\text{”}$$

$$\beta\text{-}trans\text{-}[Pt(NH_3)_2Cl_2] \rightarrow \alpha\text{-}trans\text{-}[Pt(NH_3)_2Cl_2];$$

$$fcc\text{-}Pt_xOs_{1-x} + \text{“}OsCl_4\text{”} + \alpha\text{-}trans\text{-}[Pt(NH_3)_2Cl_2] \rightarrow fcc\text{–}Pt_{0.60}Os_{0.40};$$

$$fcc\text{–}Pt_{0.60}Os_{0.40} \rightarrow fcc\text{–}Pt_yOs_{1-y}\ (\textit{major phase}) + hcp\text{–}Pt_zOs_{1-z}\ (\textit{minor phase}).$$

In inert atmosphere, thermal decomposition of $(NH_4)_2[Os_{0.40}Pt_{0.60}Cl_6]$ under ambient pressure occurs at much higher temperatures and starts above 400 °C with a direct formation of *fcc*–$Pt_{0.60}Os_{0.40}$ without any crystalline intermediates.

Thermal decomposition of $(NH_4)_2[Os_{0.40}Pt_{0.60}Cl_6]$ under high-pressure in inert (self-generated atmosphere without an addition of extra reducing agent) or reducing (H_2 fluid) environment can be considered as an alternative routine to synthesise of Os—Pt alloys. In all previous studies, alloys pre-synthetized from single-source precursors under ambient conditions were further heat-treated under high-pressure. Nevertheless, $(NH_4)_2[Os_{0.40}Pt_{0.60}Cl_6]$ can be directly decomposed under compression in piston-cylinder press, multi-anvil press, or in diamond anvil cells (Table 2). Equilibrium Os—Pt alloys were found in all experiments without a formation of any nitrides or chlorides as crystalline products. Thermal decomposition of compressed $(NH_4)_2[Os_{0.40}Pt_{0.60}Cl_6]$ powder under high hydrostatic pressure without adding any reducing agents can be considered as thermal decomposition in inert conditions. Decomposition and further annealing at 1000–2300 °C under compression results in a formation of *fcc* + *hcp* two-phase mixture. No signs of *fcc* → *hcp* or *hcp* → *fcc* transformations under compression were found below

50 GPa. Quenched unloaded sample gives an estimation for the miscibility gap under compression which does not significantly change from ambient pressure to 50 GPa (Table 2, Figures 2 and 4a).

Alternatively, ammonia borane, NH_3BH_3, as a hydrogen source, can be used for easy release of hydrogen with a formation of inert *h*–BN-like products [41]. The reaction can be reproducibly performed in a large-volume press [41]. An encapsulation of the pelletized initial single-source precursor surrounded by two ammonia borane pellets inside a NaCl capsule was performed as NaCl is inert and impermeable for hydrogen. According to the hydrogen phase diagram, hydrogen exists as supercritical fluid at 8 GPa above 375 K and at 9 GPa above 400 K [42, 43]. As a result, the reaction of single-source precursors with hydrogen fluid under high-pressure allows us to access reduction and equilibration under relatively low temperature due to high reactivity of *in statu nascendi* generated nanostructured porous metastable bimetallic particles. Hydrogen formed in the reaction vessel also should have higher reactivity and might improve reaction kinetic and equilibration.

High-pressure decomposition of $(NH_4)_2[Os_{0.40}Pt_{0.60}Cl_6]$ in hydrogen fluid occurs between 500 and 600 °C (maximal experimental temperature) without a formation of any metastable intermediate hydrides, nitrides, or chlorides. Initially formed pure *fcc*-structured phase with annealing decomposes with a formation of *fcc* + *hcp* two-phase mixture (Figure 4b, Table 2).

High-pressure high-temperature treatment of single-source precursors as well as pre-synthetized binary or multicomponent alloys may allow to prepare material unavailable under ambient pressure. Treatment under high-pressure changes thermal decomposition mechanism and increases decomposition temperature. As a result, unstable highly reactive intermediates might form. Changes of phase equilibrium in metallic systems under high-pressure should be also considered.

Conclusions

Os—Pt binary alloys have been investigated in the whole range of compositions. Existing experimental data suggest that published Os—Pt binary phase diagram should be corrected to be able to explain all experimental data. Thermal decomposition of $(NH_4)_2[Os_xPt_{1-x}Cl_6]$ under ambient and high pressure in inert and reductive atmosphere results in a formation of single and two-phase Os—Pt binary alloys. Resulting alloys after annealing correspond to equilibrium phase diagram and can be used for mapping a miscibility gap between *fcc*- and *hcp*-structured alloys. Miscibility gap between *fcc*- and *hcp*-structured alloys does not change its positions with pressure up to at least 50 GPa.

Thermal decomposition of $(NH_4)_2[Os_xPt_{1-x}Cl_6]$ under high pressure in an inert (self-generated atmosphere without adding additional reducing agent) or reducing (H_2 fluid) medium can be considered as alternative procedure for the synthesis of Os—Pt alloys. Thermal decomposition of mixed-metal $(NH_4)_2[Os_xPt_{1-x}Cl_6]$ precursor in hydrogen atmosphere (reductive environment) can be associated with a formation of β-*trans*-$[Pt(NH_3)_2Cl_2]$ and α-*trans*-$[Pt(NH_3)_2Cl_2]$ crystalline intermediates. *Fcc*-structured intermediate metallic phase with further heating or annealing decomposes with a formation of two-phase (*fcc*+*hcp*) mixture.

Detailed investigation of the thermal decomposition of pure compound $(NH_4)_2[PtCl_6]$ in hydrogen atmosphere using *in situ* X-ray diffraction and X-ray spectroscopy will give more insight into the decomposition process of mixed-metal compounds with chemically similar anions such as $[PtCl_6]^{2-}$, $[PtBr_6]^{2-}$ and $[PdCl_6]^{2-}$. Simultaneous presence of anions with different chemical properties and thermal stability such as $[OsCl_6]^{2-}$, $[IrCl_6]^{2-}$ and $[ReCl_6]^{2-}$ might drastically change thermal decomposition process.

Acknowledgements

The authors thank the ID11 and ID06-LVP beamlines at the ESRF, and P02.2 beamline at the PETRA III for providing us measurement time and technical support. We also thank Dr. Michael Hanfland (ESRF) for the help with measurements of recovered samples at the beamline ID15B, and Dr. Harald Müller (ESRF) for his kind assistance with the Chemistry Laboratory facilities at ESRF. The work was partly carried out in accordance with the state assignment for the Institute of Solid State Chemistry of the Ural Brunch of Russian Academy of Sciences (theme No AAAA-A19-119031890025-9).

References

[1] L.D. Blackburn, L. Kaufman, M. Cohen, Phase Transformations in Iron-Ruthenium alloys under high pressure. Acta Metallurg. 13 (1965), 533-541. DOI: 10.1016/0001-6160(65)90104-5

[2] I. Halevy, S. Salhov, M.L. Winterrose, A. Broide, A.F. Yue, A. Robin, O. Yeheskel, J. Hu, I. Yaar, High pressure study and electronic structure of the super-alloy $HfIr_3$. J. Phys.: Conf. Ser., 215(1) (2010), 012012. doi:10.1088/1742-6596/215/1/012012

[3] K.V. Yusenko, E. Bykova, M. Bykov, S.A. Gromilov, A.V. Kurnosov, C. Prescher, V.B. Prakapenka, M. Hanfland, S. van Smaalen, S. Margadonna, L.S. Dubrovinsky, Compressibility of Ir─Os alloys under high pressure. J. Alloys and Comp., 622 (2015), 155 DOI: 10.1016/j.jallcom.2014.09.210

[4] K.V. Yusenko, E. Bykova, M. Bykov, S.A. Gromilov, A.V. Kurnosov, C. Prescher, V.B. Prakapenka, W.A. Crichton, M. Hanfland, S. Margadonna, L.S. Dubrovinsky, High-pressure high-temperature stability of hcp-Ir_xOs_{1-x} (x = 0.50 and 0.55) alloys. J. Alloys and Comp., 700 (2017), 198–207 10.1016/j.jallcom.2016.12.207

[5] K.V. Yusenko, E. Bykova, M. Bykov, S. Riva, W.A. Crichton, M.V. Yusenko, A.S. Sukhikh, S. Arnaboldi, M. Hanfland, L.S. Dubrovinsky, S.A. Gromilov, Ir—Re binary alloys under extreme conditions and their electrocatalytic activity in methanol oxidation. Acta Materialia, 139 (2017), 236–243. https://doi.org/10.1016/j.actamat.2017.08.012

[6] L. Dubrovinsky, N. Dubrovinskaia, V.B. Prakapenka, A.M. Abakumov, Implementation of micro-ball nanodiamond anvils for high-pressure studies above 6 Mbar. Nat. Commun. 3(1163) (2012), 1–7. DOI: 10.1038/ncomms2160.

[7] L. Dubrovinsky, N. Dubrovinskaia, E. Bykova, M. Bykov, V. Prakapenka, C. Prescher, K. Glazyrin, H.-P. Liermann, M. Hanfland, M. Ekholm, Q. Feng, L.V. Pourovskii, M.I. Katsnelson, J.M. Wills, I.A. Abrikosov, The most incompressible metal osmium at static pressures above 750 gigapascals. Nature, 525 (2015), 226–229. DOI: 10.1038/nature14681

[8] B.K. Godwal, J. Yan, S.M. Clark, R. Jeanloz, High-pressure behaviour of osmium: An analog for iron in Earth's core, J. Appl. Phys., 111 (2012), 112608. DOI: 10.1063/1.4726203

[9] R.O.C. Fonseca, V. Laurenz, G. Mallmann, A. Luguet, N. Hoehne, K.P. Jochum, New constraints on the genesis and long-term stability of Os-rich alloys in the Earth's mantle, Geochim. Cosmochim. Acta, 87 (2012), 227-242. DOI: 10.1016/j.gca.2012.04.002

[10] N. Dimakis, F.A. Flor, N.E. Navarro, A. Salgado, E.S. Smotkin, Adsorption of Carbon Monoxide on Platinum−Ruthenium, Platinum−Osmium, Platinum−Ruthenium−Osmium, and Platinum− Ruthenium−Osmium−Iridium Alloys. J. Phys. Chem. C, 120 (2016), 10427−10441. https://doi.org/10.1021/acs.jpcc.6b02086

[11] Renxuan Liu, Hakim Iddir, Qinbai Fan Gouyan Hou, Aili Bo, K.L. Ley, E.S. Smotkin, Y.-E. Sung, H. Kim, S. Thomas, A. Wieckowski, Potential-Dependent Infrared Absorption Spectroscopy of Adsorbed CO and X-ray Photoelectron Spectroscopy of Arc-Melted Single-Phase

Pt, PtRu, PtOs, PtRuOs, and Ru Electrodes. J. Phys. Chem. B, 104 (2000), 3518–3531. https://doi.org/10.1021/jp992943s

[12] Ho-Cheng Tsai, Yu-Chi Hsieh, Yu, T.H., Yi-Juei Lee, Yue-Han Wu, B.V. Merinov, Pu-Wei Wu, San-Yuan Chen, R.R. Adzic, W.A. Goddard III, DFT Study of Oxygen Reduction Reaction on Os/Pt Core–Shell Catalysts Validated by Electrochemical Experiment. ACS Catal., 5 (2015), 1568–1580. https://doi.org/10.1021/cs501020a

[13] B. Gurau, R. Viswanathan, Renxuan Liu, T.J. Lafrenz, K.L. Ley, E.S. Smotkin, E. Reddington, A. Sapienza, B.C. Chan, T.E. Mallouk, S. Sarangapani, Structural and Electrochemical Characterization of Binary, Ternary, and Quaternary Platinum Alloy Catalysts for Methanol Electro-oxidation. J. Phys. Chem. B, 102 (1998), 9997–10003. https://doi.org/10.1021/jp982887f

[14] I.V. Korolkov, A.I. Gubanov, K.V. Yusenko, I.A. Baidina, S.A. Gromilov, Synthesis of non-equilibrium PtxOs1-x solid solutions. Crystal structure of $[Pt(NH_3)_4][OsCl_6]$. J. Struct. Chem., 48(3) (2007), 486–493. DOI: 10.1007/s10947-007-0073-1

[15] S.A. Gromilov, T.V. D'yachkova, A.P. Tyutyunnik, Yu.G. Zainulin, A.I. Gubanov, S.V. Cherepanova, The product of thermobaric treatment of $Pt_{0.25}Os_{0.75}$. J. Struct. Chem. 49 (2008), 382–385. https://doi.org/10.1007/s10947-008-0138-9

[16] P. Rajiv, R. Dinnebier, M. Jansen, Powder 3D Parametric: A program for automated sequential and parametric Rietveld refinement using Topas. Materials Science Forum 651 (2010) 97–104.

[17] T. Grützner, S. Klemme, A. Rohrbach, F. Gervasoni, J. Berndt, The effect of fluorine on the stability of wadsleyite: Implications for the nature and depths of the transition zone in the Earth's mantle. Earth Planet. Sci. Lett. 482 (2018), 236–244. https://doi.org/10.1016/j.epsl.2017.11.011

[18] J. Guignard and W. A. Crichton, The large volume press facility at ID06 beamline of the European synchrotron radiation facility as a High Pressure-High Temperature deformation apparatus. Rev. Sci. Instrum. 86 (8) (2015) 085112. doi: 10.1063/1.4928151

[19] F. Birch, Equation of state and thermodynamic parameters of NaCl to 300 kbar in the high-temperature domain. JGR Solid Earth. 91 (1986), 4949–4954. https://doi.org/10.1029/JB091iB05p04949

[20] A. P. Hammersley, S. O. Svensson, M. Hanfland, A. N. Fitch, and D. Häusermann, Two-Dimensional Detector Software: From Real Detector to Idealised Image or Two-Theta Scan. High Press. Res., 14 (1996), 235-248. DOI: 10.1080/08957959608201408

[21] K. Anbukumaran, C. Venkateswaran, N.V. Jaya, S. Natarajan, Piston-cylinder apparatus for high-pressure and high-temperature studies. High-Press. Sci. Techn., 1-2 (1994), 1585–1588.

[22] H.-P. Liermann, Z. Konopkova, W. Morgenroth, K. Glazyrin, J. Bendarchik, E.E. McBride, S. Petitgirard, J.T. Delitz, M. Wendt, Y. Bican, A. Ehnes, I. Schwark, A. Rothkirch, M. Tischer, J. Heuer, H. Schulte-Schrepping, T. Kracht, H. Franz, The extreme conditions beamline P02.2 and the extreme conditions science infrastructure at PETRA III. J. Synchrotron Radiation, 22 (2015), 908–924. DOI: 10.1107/S1600577515005937

[23] C. Prescher, V.B. Prakapenka, DIOPTAS: a program for reduction of two-dimensional X-ray diffraction data and data exploration. High Press. Res., 35 (2015), 223–230. https://doi.org/10.1080/08957959.2015.1059835

[24] V. Petricheck, M. Duscheck, L. Palatinus, Jana2006. The crystallographic computing system. –Institute of Physics. – Praha, Czech Republic. – 2006; http://www-xray.fzu.cz/jana/jana.html

[25] L.I. Voronova, V.P. Polyakova, E.M. Savitskii, Alloys of the System Pt—Os. Izvestiya Akademii Nauk SSSR, Metals., 5 (1984), 191–193

[26] R.S. Rudman, Lattice parameters of some h.c.p. binary alloys of rhenium and osmium: Re-W, Re-Ir, Re-Pt; Os-Ir, Os-Pt, J. Less-Common Metals. 12(1) (1967), 79-81. DOI: 10.1016/0022-5088(67)90075-6

[27] Powder Diffraction File. Alphabetical Index. Inorganic Phases, JCPDS, International Centre for Diffraction Data, Pennsylvania, USA, 1983, 1023 p.

[28] A.I. Gubanov, A.I. Double complex salts with tetraammine cations as precursors for metallic powders. PhD Thesis, Nikolaev Institute of Inorganic Chemistry, Novosibirsk, Russian Federation, 2003, 21 p. (in Russian: Губанов А.И. Двойные комплексы с тетраамминными катионами – предшественники металлических порошков. Автореферат диссертации на соискание ученой степени к.х.н. Новосибирск, 2003. 21 С.)

[29] T.I. Asanova, I.P. Asanov, M.-G. Kim, S.V. Korenev, In situ X-ray spectroscopic investigation of thermal decomposition of double complex salt $[Pt(NH_3)_4][OsCl_6]$. J. Struct. Chem. 58 (2017), 901–910. https://doi.org/10.1134/S0022476617050079

[30] S.-L. Chen, S. Daniel, F. Zhang, Y.A. Chang, X.-Y. Yan, F.-Y. Xie, R. Schmid-Fetzer, W.A. Oates, The Pandat Software Package and its Applications. CALPHAD, 26 (2002), 175–188. https://doi.org/10.1016/S0364-5916(02)00034-2

[31] A.T. Dinsdale, SGTE data for pure elements. CALPHAD, 15 (1991), 317–425. https://doi.org/10.1016/0364-5916(91)90030-N

[32] Chang-Sheng Zha, K. Mibe, W.A. Basset, O. Tschauner, Ho-Kwang Mao, R.J. Hemley, P—V—T equation of state of platinum to 80 GPa and 1900 K from internal resistive heating/x-ray diffraction measurements. J. Appl. Phys., 103 (2008), 054908. https://doi.org/10.1063/1.2844358

[33] S.A. Gromilov, Yu.V. Shubin, A.I. Gubanov, E.A. Maksimovskii, S.V. Korenev, X-ray study of the thermolysis products of $(NH_4)_2[OsCl_6]_x[PtCl_6]_{1-x}$. J. Struct. Chem., 50 (2009), 1121–1125. https://doi.org/10.1007/s10947-009-0164-2

[34] Q. Kong, F. Baudelet, J. Han, S. Chagnot, L. Barthe, J. Headspith, R. Goldsbrough, F.E. Picca, O. Spalla, Microsecond time-resolved energy-dispersive EXAFS measurement and its application to film the thermolysis of $(NH_4)_2[PtCl_6]$. Sci. Rep. 2012, 2, 1018. doi: 10.1038/srep01018

[35] H. Rumpf, J. Hormes, A. Moller, G. Meyer, Thermal decomposition of $(NH_4)_2[PtCl_6]$ – an *in situ* X-ray absorption spectroscopy study. J. Synchrotron Rad., 6 (1999), 468–470. DOI: 10.1107/S0909049598015994

[36] G. Meyer, A. Moller, Thermolysis of ternary ammonium chlorides of rhenium and the noble-metals. J. Less-Common Met., 170 (1991), 327–331. https://doi.org/10.1016/0022-5088(91)90336-3

[37] G. Matuschek, K.H. Ohrbach, A. Kettrup, Simultaneous thermal-analysis mass-spectrometric investigations on the thermal behaviour of noble-metal complexes. Thermochim. Acta, 190 (1991), 125–130. https://doi.org/10.1016/0040-6031(91)85238-D

[38] Y. Verde-Gomez, G. Alonso Nunez, F. Cervantes, A. Keer, Aqueous solution reaction to synthesize ammonium hexachloroplatinate and its crystallographic and thermogravimetric characterization. Mater. Lett., 57 (2003), 4667–4672. https://doi.org/10.1016/S0167-577X(03)00381-1

[39] R.D. Weir, E.F. Westrum, Thermodynamics, phase transitions and crystal structure of ammonium hexahalides: comparative study of the heat capacity and thermodynamic properties of $(NH_4)_2PtCl_6$, $(ND_4)_2PtCl_6$, $(NH_4)_2PtBr_6$, $(ND_4)_2PtBr_6$, $(NH_4)_2PdCl_6$, $(ND_4)_2PdCl_6$, $(NH_4)_2TeCl_6$,

$(ND_4)_2TeCl_6$, and $(NH_4)_2RuCl_6$ from 5 K to 350 K. J. Chem. Thermodynamics, 34 (2002), 133–153. doi:10.1006/jcht.2001.0910

[40] S.A. Gromilov, S.P. Khranenko, I.A. Baidina, A.V. Belyaev, Synthesis and crystal structure refinement of β-trans-$[Pd(NH_3)_2Cl_2]$. Russ. J. Inorg. Chem., 45 (2000), 1354–1359.

[41] D.Yu. Naumov, S.P. Khranenko, N.V. Kuratieva, A.V. Panchenko, S.A. Gromilov, New data on the structure of α-trans-$[Pd(NH_3)_2Cl_2]$. J. Struct. Chem., 57 (2016), 1600–1605. https://doi.org/10.1134/S0022476616080163

[42] J. Nylén, T. Sato, E. Soignard, J.A. Yarger, E. Stoyanov, U. Häussermann, Thermal decomposition of ammonia borane at high pressures. J. Chem. Phys., 131 (2009), 104506. https://doi.org/10.1063/1.3230973

[43] C.-S. Zha, H. Liu, J.S. Tse, R.J. Hemley, Melting and High P—T Transitions of Hydrogen up to 300 GPa. Phys. Rev. Lett., 119 (2017), 075302. https://doi.org/10.1103/PhysRevLett.119.075302

[44] V. Diatschenko, C.W. Chu, D.H. Liebenberg, D.A. Young, M. Ross, R.L. Mills, Melting curves of molecular hydrogen and molecular deuterium under high pressures between 20 and 373 K. Phys. Rev. B, 32 (1985), 381. DOI: 10.1103/physrevb.32.381

Figure 1. Phase diagram of Os—Pt binary system (*right axis*): experimental data from [25] (*stars*) and modelled phase diagram using ideal solutions model (*dashed line*). Hexagons (*hcp*-structured Os—Pt alloys) and squares (*fcc*-structured Os—Pt alloys) correspond to atomic volumes of single-phase Os—Pt binary alloys according to Table 1 (*left axis*).

Figure 2. Pressure-dependence of the phase miscibility for Os—Pt alloys with pressure below 20 GPa at temperature above 1000 °C. *Hexagons* (*hcp*-structured Os—Pt alloys) and *squares* (*fcc*-structured Os—Pt alloys) correspond to Table 2, circles correspond to starting composition before heat-treatment. Open hexagons and squares correspond to annealed two-phase samples.

Figure 3. Thermal decomposition of $(NH_4)_2[Os_{0.40}Pt_{0.60}Cl_6]$ (shown as s) (ambient pressure, ESRF-ID-11, Ar (A) and 2 vol.% H_2/Ar flow (B), 12 K/min heating rate, λ = 0.3086 Å). Representations of possible crystal structures of β-*trans*-$[Pt(NH_3)_2Cl_2]$ (shown as *bt*) along *b*-axis (C) and α-*trans*-$[Pt(NH_3)_2Cl_2]$ (shown as *at*) along *c*-axis (D) based on their Pd-containing analogues (see text for details).

Figure 4. Thermal decomposition of $(NH_4)_2[Os_{0.40}Pt_{0.60}Cl_6]$ under high-pressure in diamond anvil cell (*Left*: PETRA III – P02.2 PETRA III, 20-40 GPa, Ne as pressure-transmitting medium, λ = 0.2907 Å, *s* stands for $(NH_4)_2[Os_{0.40}Pt_{0.60}Cl_6]$ precursor salt, *g* stands for Re gasket) and in the large-volume press in hydrogen fluid at 8.5 GPa from 300 °C to 600 °C (ESRF – ID06-LVP, λ = 0.2254 Å, *s* corresponds to $(NH_4)_2[Os_{0.40}Pt_{0.60}Cl_6]$ precursor salt, *fcc* – correspond to *fcc*-$Os_{0.40}Pt_{0.60}$, other diffraction lines correspond to assembly).

Table 1. Single-phase Os—Pt alloys

Table 2. Thermobaric treatment of Os—Pt alloys and $(NH_4)_2[Os_xPt_{1-x}Cl_6]$ single-source precursors

Table 1. Single-phase Os—Pt alloys

Composition Ref.	*a*, Å *c*, Å	*V*/*Z*, Å^3·atom^{-1}	d_x, g/cm^3	Preparatory conditions
hcp-phases ($P6_3/mmc$)				
hcp-Os [27, №6-662]	2.7341(2) 4.3197(4)	13.98	22.587	Reference material
hcp-$Os_{0.95}Pt_{0.05}$ [26]	2.7350(7) 4.322(12)	14.00	22.587	Sintering 1 h, 2500 °C
hcp-$Os_{0.90}Pt_{0.10}$ [26]	2.7361(7) 4.3247(12)	14.02	22.585	Sintering, 1 h, 2500 °C
hcp-$Os_{0.90}Pt_{0.10}$ [14]	2.738(2) 4.346(3)	14.11	22.440	Thermal decomposition of $(NH_4)_2[Os_{0.90}Pt_{0.10}Cl_6]$, 550 °C, H_2
hcp-$Os_{0.80}Pt_{0.20}$ [14]	2.735(2) 4.375(3)	14.17	22.401	Thermal decomposition of $(NH_4)_2[Os_{0.80}Pt_{0.20}Cl_6]$, 550 °C, H_2
hcp-$Os_{0.75}Pt_{0.25}$ (Sample A) [15]	2.736(1) 4.391(2)	14.23	22.336	Thermal decomposition of $(NH_4)_2[Os_{0.75}Pt_{0.25}Cl_6]$, 550 °C, H_2
fcc-phases ($Fm\bar{3}m$)				
fcc-$Os_{0.50}Pt_{0.50}$ [28]	3.899(3)	14.82	21.586	Thermal decomposition of $[Pt(NH_3)_4][OsCl_6]$, 600 °C, He
fcc-$Os_{0.50}Pt_{0.50}$ [28]	3.899(3)	14.82	21.586	Thermal decomposition of $[Pt(NH_3)_4][OsBr_6]$, 500 °C, H_2
fcc-$Os_{0.50}Pt_{0.50}$ [14]	3.91(1)	14.98	21.356	Thermal decomposition of $[Pt(NH_3)_4][OsCl_6]$, 500 °C, He
fcc-$Os_{0.30}Pt_{0.70}$ [14]	3.898(3)	14.81	21.713	Thermal decomposition of $(NH_4)_2[Os_{0.30}Pt_{0.70}Cl_6]$, 500 °C, H_2
fcc-$Os_{0.25}Pt_{0.75}$ (Sample B) [14]	3.902(3)	14.85	21.673	Thermal decomposition of $(NH_4)_2[Os_{0.25}Pt_{0.75}Cl_6]$, 500 °C, He
fcc-$Os_{0.20}Pt_{0.80}$ [26]	3.9049(7)	14.89	21.652	Sintering, 1 h, 1700 °C
fcc-$Os_{0.10}Pt_{0.90}$ [26]	3.9127(7)	14.98	21.577	Sintering, 1 h, 1700 °C
fcc-Pt [27, №4-802]	3.9231(2)	15.09	21.460	Reference material

Table 2. Thermobaric treatment of Os—Pt alloys and $(NH_4)_2[Os_xPt_{1-x}Cl_6]$ single-source precursors

Nominal composition	Phase composition after thermobaric treatment	*a*, Å *c*, Å	*V*/*Z*, Å^3·atom^{-1}	Experimental conditions
$Os_{0.40}Pt_{0.60}$ EDX 30/70 [33]	*hcp*-$Os_{0.89}Pt_{0.71}$	2.737(2) 4.370(4)	14.18(4)	$(NH_4)_2[Os_{0.40}Pt_{0.60}Cl_6]$ ambient pressure, H_2 flow, 400 °C, 15 min
	fcc-$Os_{0.89}Pt_{0.71}$	3.898(2)	14.82(5)	
$Os_{0.50}Pt_{0.50}$ EDX = 40/60 [33]	*hcp*-$Os_{0.76}Pt_{0.24}$	2.739(2) 4.372(4)	14.20(4)	$(NH_4)_2[Os_{0.50}Pt_{0.50}Cl_6]$, ambient pressure, H_2 flow, 400 °C, 15 min
	fcc-$Os_{0.37}Pt_{0.63}$	3.895(2)	14.77(5)	
$Os_{0.60}Pt_{0.40}$ EDX = 55/45 [15, 33]	23 at. % *hcp*-$Os_{0.73}Pt_{0.27}$	2.741(4) 4.374(8)	14.23(8)	$(NH_4)_2[Os_{0.60}Pt_{0.40}Cl_6]$ ambient pressure, H_2 flow, 400 °C, 15 min
	77 at. % *fcc*-$Os_{0.32}Pt_{0.68}$	3.897(3)	14.80(8)	
$Os_{0.40(3)}Pt_{0.60(3)}$ EDX Os/Pt = 40(3)/60(3) [Current study]	13 at. % *hcp*-$Os_{0.82}Pt_{0.18}$	2.740(2) 4.347(4)	14.132(5)	Decomposition of $(NH_4)_2[Os_{0.40}Pt_{0.60}Cl_6]$, 1 GPa, 1000 °C, 80 min
	87 at. % *fcc*-$Os_{0.02}Pt_{0.98}$	3.920(2)	15.059(5)	
hcp-$Os_{0.75}Pt_{0.25}$ (EDX: Os/Pt = 69/31) [15]	41 at. % *hcp*-$Os_{0.87}Pt_{0.13}$	2.737(2) 4.340(4)	14.08(4)	Annealing *hcp*-$Os_{0.75}Pt_{0.25}$ Sample A, 1.5-2 GPa, 2000 °C, 3 min
	59 at. % *fcc*-$Os_{0.54}Pt_{0.46}$	3.888(2)	14.69(5)	
$Os_{0.25}Pt_{0.75}$ [Current study]	*fcc*-$Os_{0.25}Pt_{0.75}$	3.895(2)	14.77(5)	$Pt_{0.75}Os_{0.25}$ (a = 3.902(3) Å) Sample B, 4 GPa, 2000 °C, 3 min
$Os_{0.40(3)}Pt_{0.60(3)}$ EDX Os/Pt = 40(3)/60(3) [Current study]	5 at. % *hcp*-$Os_{0.73}Pt_{0.27}$	2.741(2) 4.374(4)	14.230(2)	Decomposition of $(NH_4)_2[Os_{0.40}Pt_{0.60}Cl_6]$ H_2 fluid 8.5-9 GPa, 600 °C, 30 min
	95 at. % *fcc*-$Os_{0.35}Pt_{0.65}$	3.896(1)	14.784(2)	
$Os_{0.5}Pt_{0.5}$ [Current study]	24 at. % *hcp*-$Os_{0.89}Pt_{0.11}$	2.73592(9) 4.34134(19)	14.071(2)	Decomposition of $(NH_4)_2[Os_{0.50}Pt_{0.50}Cl_6]$, 10 GPa, 2000 °C, 5 min
	76 at. % *fcc*-$Os_{0.41}Pt_{0.59}$	3.88136(10)	14.618(2)	
$Os_{0.5}Pt_{0.5}$ [Current study]	85 at. % *fcc*-$Os_{0.43}Pt_{0.57}$	3.879(2)	14.591(5)	Decomposition of $(NH_4)_2[Os_{0.50}Pt_{0.50}Cl_6]$, 18 GPa, 1200 °C, 2 min
	15 at. % *fcc*-$Os_{0.82}Pt_{0.18}$	3.840(2)	14.156(5)	
$Os_{0.5}Pt_{0.5}$ [Current study]	5 at. % *hcp*-$Os_{0.74}Pt_{0.26}$	2.742(2) 4.378(4)	14.252(5)	Decomposition of $(NH_4)_2[Os_{0.50}Pt_{0.50}Cl_6]$ at 24 GPa and 2300 °C, further laser-heating at 30, 40 and 50 GPa up to 2000, 1600 and 850 °C, respectively
	95 at. % *fcc*-$Os_{0.35}Pt_{0.65}$	3.888(2)	14.689(5)	

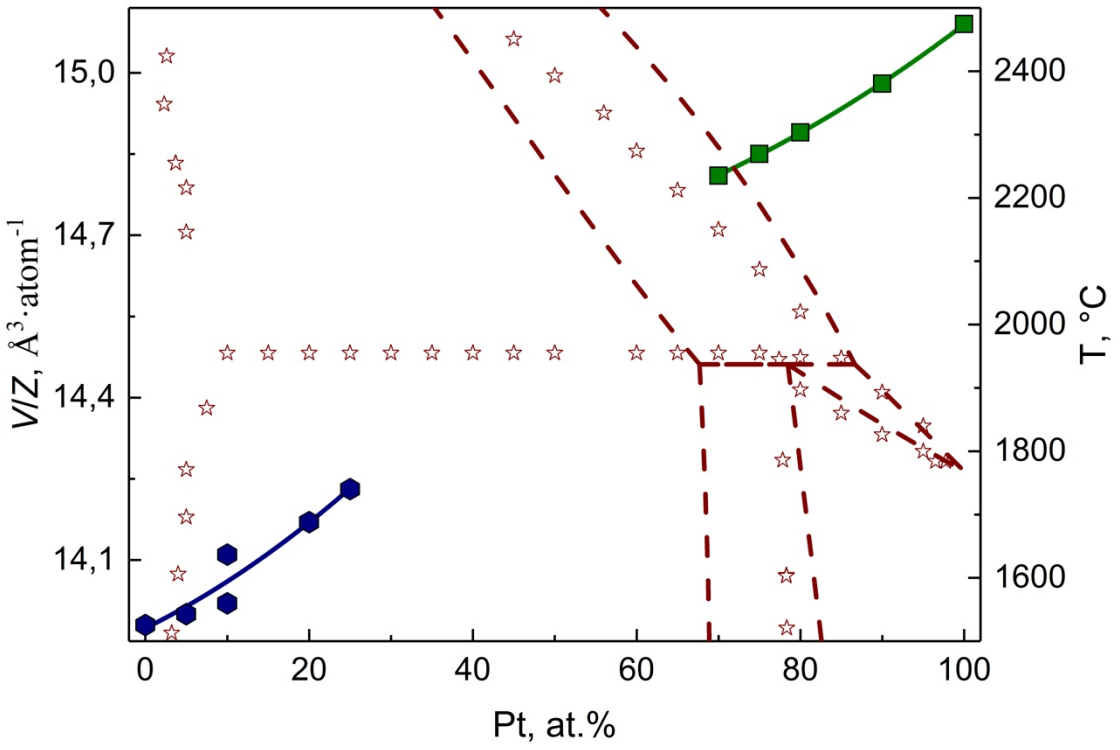

Figure 1. Phase diagram of Os—Pt binary system (*right axis*): experimental data from [25] (*stars*) and modelled phase diagram using ideal solutions model (*dashed line*). Hexagons (*hcp*-structured Os—Pt alloys) and squares (*fcc*-structured Os—Pt alloys) correspond to atomic volumes of single-phase Os—Pt binary alloys according to Table 1 (*left axis*).

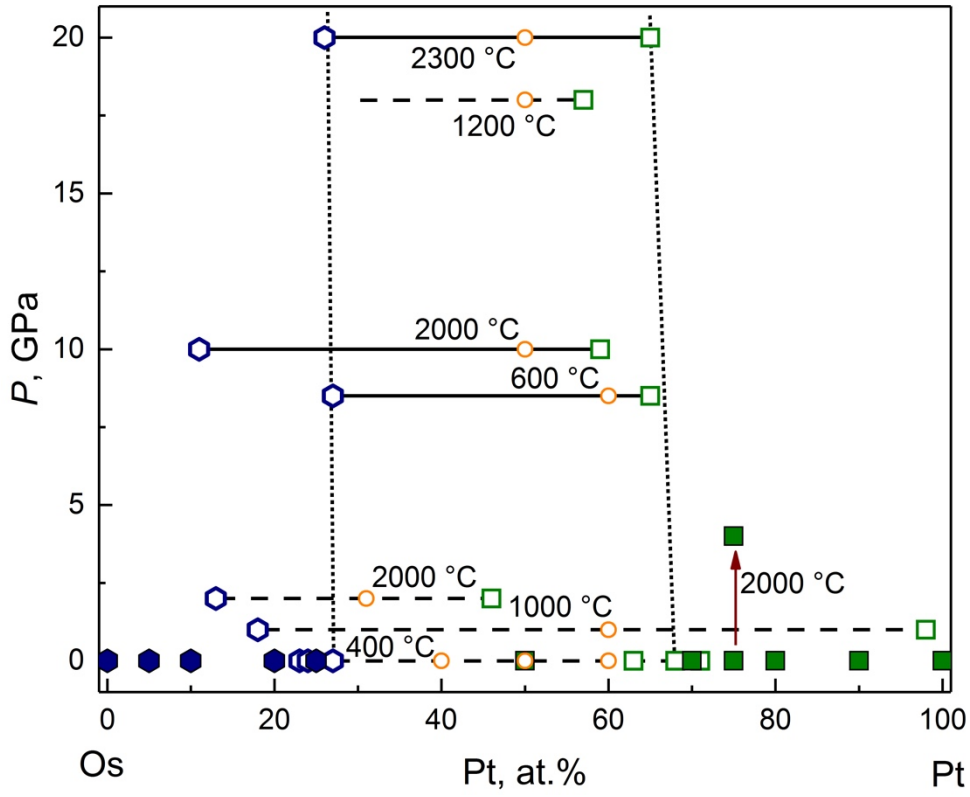

Figure 2. Pressure-dependence of the phase miscibility for Os—Pt alloys with pressure below 20 GPa at temperature above 1000 °C. *Hexagons* (*hcp*-structured Os—Pt alloys) and *squares* (*fcc*-structured Os—Pt alloys) correspond to Table 2, circles correspond to starting composition before heat-treatment. Open hexagons and squares correspond to annealed two-phase samples.

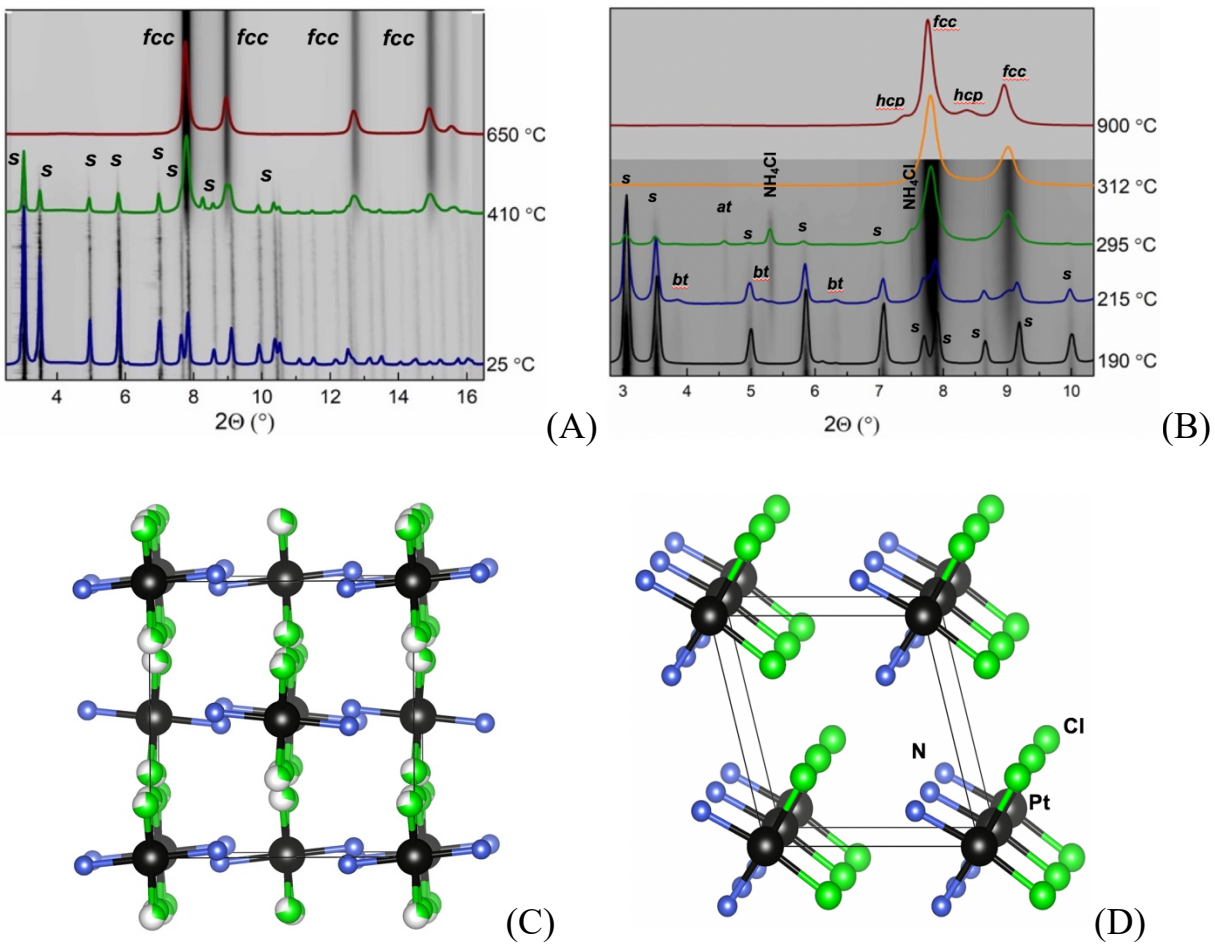

Figure 3. Thermal decomposition of $(NH_4)_2[Os_{0.40}Pt_{0.60}Cl_6]$ (shown as s) (ambient pressure, ESRF-ID-11, Ar (A) and 2 vol.% H_2/Ar flow (B), 12 K/min heating rate, λ = 0.3086 Å). Representations of possible crystal structures of β-*trans*-$[Pt(NH_3)_2Cl_2]$ (shown as *bt*) along *b*-axis (C) and α-*trans*-$[Pt(NH_3)_2Cl_2]$ (shown as *at*) along *c*-axis (D) based on their Pd-containing analogues (see text for details).

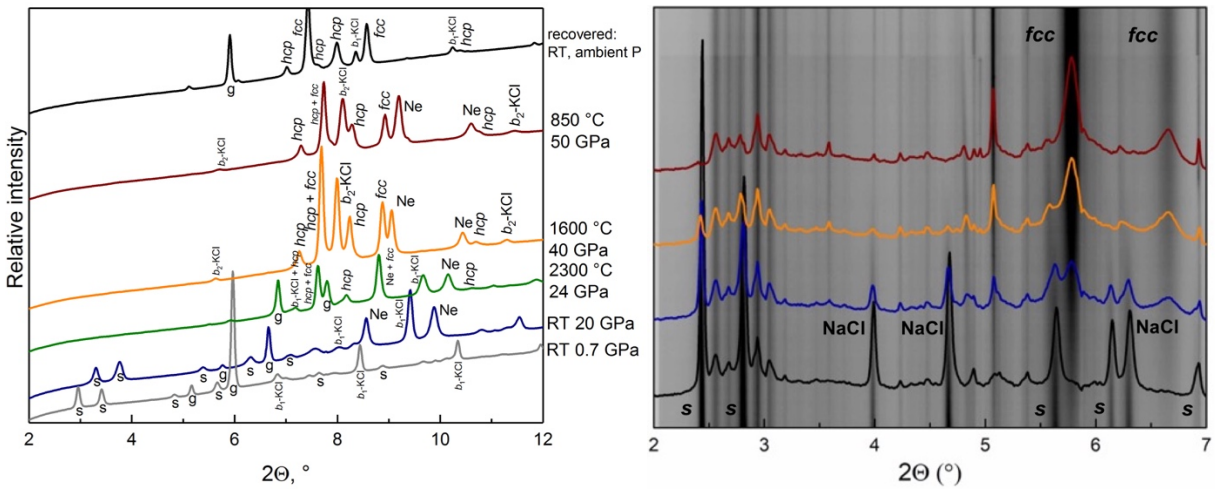

Figure 4. Thermal decomposition of $(NH_4)_2[Os_{0.40}Pt_{0.60}Cl_6]$ under high-pressure in diamond anvil cell (*Left*: PETRA III – P02.2 PETRA III, 20-40 GPa, Ne as pressure-transmitting medium, λ = 0.2907 Å, *s* stands for $(NH_4)_2[Os_{0.40}Pt_{0.60}Cl_6]$ precursor salt, *g* stands for Re gasket) and in the large-volume press in hydrogen fluid at 8.5 GPa from 300 °C to 600 °C (ESRF – ID06-LVP, λ = 0.2254 Å, *s* corresponds to $(NH_4)_2[Os_{0.40}Pt_{0.60}Cl_6]$ precursor salt, *fcc* – correspond to *fcc*-$Os_{0.40}Pt_{0.60}$, other diffraction lines correspond to assembly).